

Modelling of thermodynamics and diffusion in multicomponent systems

U. R. Kattner* and C. E. Campbell

The availability of reliable materials data is key to the successful design of materials and manufacturing processes. Commercial alloys seldom consist of only two or three elements, but rather may contain a large number of elements for which the needed data are rarely available. The CALPHAD (calculation of phase diagrams method), as implemented in a number of software tools, enables the development of thermodynamic and diffusion databases and the extrapolation of these property data from binary and ternary systems to higher order systems. The computational methods used to calculate thermodynamic and diffusion properties can be invaluable in the design of new materials. In addition, the databases and software tools provide an efficient method of storing a wealth of data and allow efficient retrieval of the needed information. The present paper reviews the development and application of multicomponent thermodynamic and diffusion mobility databases using the CALPHAD method.

Keywords: CALPHAD, Databases, Diffusion, Phase equilibria, Thermodynamics

Introduction

Accurate prediction of microstructure evolution during processing and service is essential to successful materials design. The fundamental inputs for accurate microstructure prediction are phase equilibria data and diffusion mobility data. Although phase diagrams do not provide information about kinetic processes, they may give information on the potential for the formation of metastable states. Diffusion determines the rate by which equilibrium is reached from a non-equilibrium state. As both the phase equilibria and diffusion mobility data depend on composition, temperature and pressure, the amount of data needed for a multicomponent system quickly becomes overwhelming. The calculation of phase diagrams (CALPHAD) method applied to both of these data sets provides an efficient method to store and represent needed data, as well as a method to extrapolate to higher order systems.

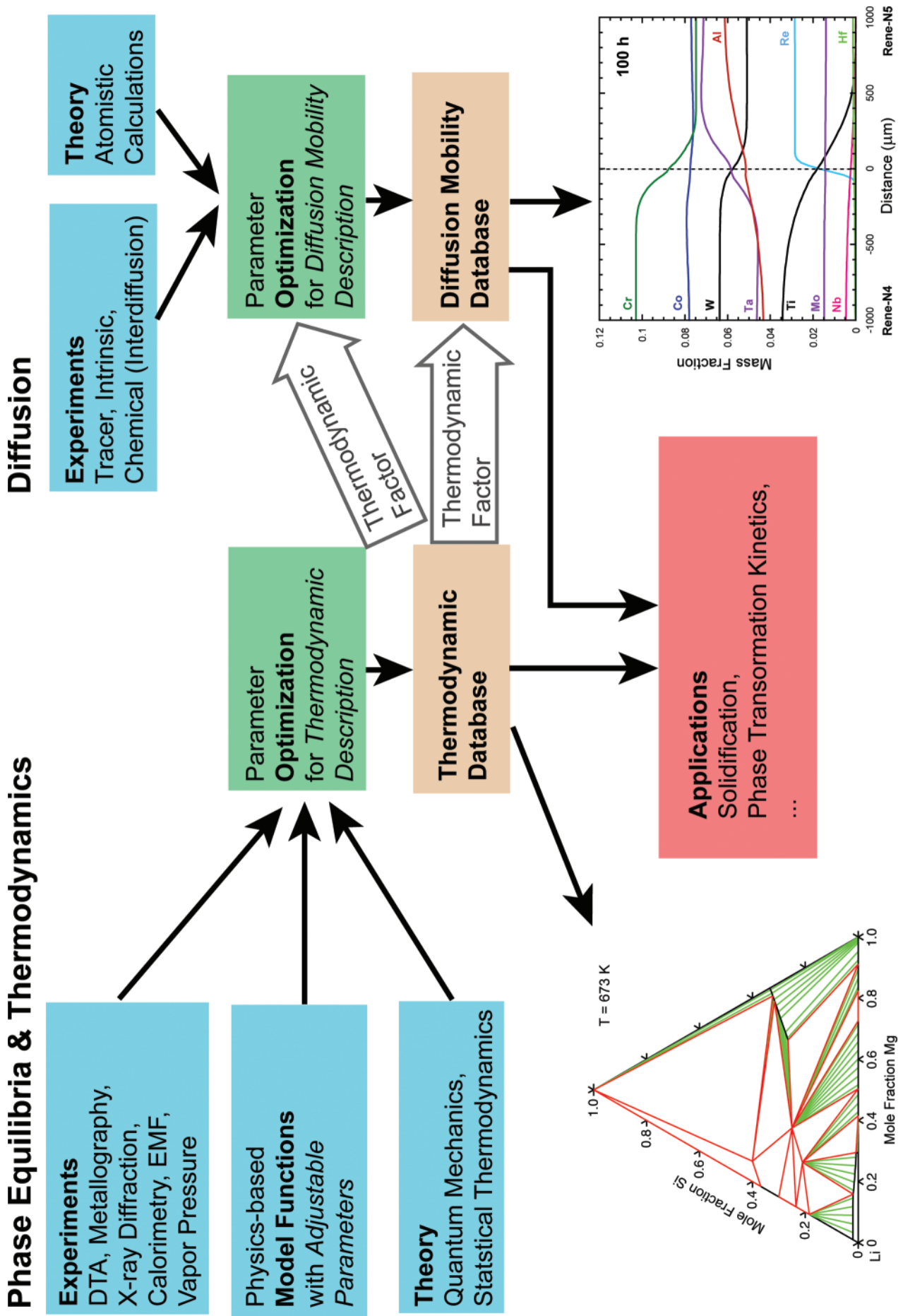
The importance of phase equilibria and their visual representation in the form of phase diagrams for alloy design, development, processing and understanding is reflected by a large number of phase diagram compilations. Traditionally these compilations were published in the form of handbooks, such as 'Binary alloy phase diagrams',¹ 'Phase equilibria, crystallographic and thermodynamic data of binary alloys',² 'Phase equilibrium diagrams',³ which continues 'Phase diagrams for ceramists',⁴ 'Handbook of Ternary alloy phase diagrams',⁵ and 'Ternary alloys',⁶ and a large number of books that focus on systems with a specific base element.

In recent years, searchable CD-ROM versions of some of these phase diagram handbooks or searchable online databases have become available.⁷⁻⁹ For all of these media the phase diagrams are represented as two-dimensional (2D) diagrams. This is fairly straightforward for a binary system, which can be represented for constant pressure by a temperature concentration ($T-x$) diagram. However, for systems with more than two components, the addition of a component requires one more dimension to display the phase diagram. Therefore, multicomponent systems are commonly represented by a series of projections and sections in two-dimensions. This multidimensionality makes the interpretation of these multicomponent diagrams quite cumbersome for an occasional user of these diagrams. In addition to the difficult graphical representation of multicomponent systems, these systems also frequently lack sufficient experimental information to construct the multidimensional diagrams.

Diffusion coefficients describe the rate of flux of a particular component through a material and, when combined with phase equilibria data, enable the prediction of microstructure evolution. Traditional compilations of diffusion data include diffusion data in pure and binary materials. Examples of some of these compilations include Smithells,¹⁰ Landolt-Börnstein series,¹¹ Diffusion and Defect Forum,¹² and the National Institute of Standards and Technology (NIST) Diffusion Data Center.¹³ Diffusion data for higher order systems, with n components in the system, become increasingly more difficult to obtain as $(n-1)$ composition profiles with different terminal compositions intersecting at a common point are needed to determine a single diffusion coefficient. Experimentally determining all the needed diffusion coefficient matrixes for a

Metallurgy Division, National Institute of Standards and Technology, 100 Bureau Dr Stop 8555, Gaithersburg MD 20899, USA

*Corresponding author, email ursula.kattner@nist.gov



1 Schematic of CALPHAD method

multicomponent diffusion simulation is simply not practical or efficient.

The difficulties in representing multicomponent phase diagrams and determining multicomponent diffusion coefficients are overcome by using the CALPHAD method to calculate specific quantities for a material of interest. The CALPHAD method enables the extrapolation of phase diagram and multicomponent diffusion data in a consistent manner when no, or insufficient, experimental information is available. While modern developments in modelling and computational technology have made computer calculations of multicomponent phase equilibria a realistic possibility, the correlation between thermodynamics and phase equilibria was established more than a century ago by Gibbs (*see* Hertz¹⁴ for a summary). Detailed overviews of the CALPHAD method and its applications are given by Kaufman and Bernstein¹⁵ and more recently by Saunders and Miodownik.¹⁶ The history of CALPHAD is described by Spencer.¹⁷

Ågren^{18,19} suggested the use of the CALPHAD method for developing diffusion mobility databases to facilitate efficient calculation of multicomponent diffusion coefficients. Ågren and co-workers^{20–23} demonstrated that diffusion mobility databases can be developed assuming that a vacancy exchange mechanism occurs in crystalline phase with an equilibrium vacancy concentration, and that all the phenomenological diffusion coefficients can be expressed in terms of a diffusion mobility function and a thermodynamic factor. The presumption is that the thermodynamic factor, which is determined using an existing multicomponent thermodynamic database, has the strongest composition dependence and provides the correct behaviour of the multicomponent off diagonal diffusion coefficients as the binary solutions are approached. The use of the CALPHAD method to develop diffusion mobility databases has become crucial in numerical simulations of diffusion processes for multicomponent alloys where composition and temperature dependent diffusion coefficient matrixes are needed for each grid point after each time step.

Thermodynamic and diffusion mobility databases developed using the CALPHAD method provide an efficient representation of the composition and temperature dependences in multicomponent systems. The schematic in Fig. 1 reviews how experimental data and theory are integrated to develop thermodynamic and diffusion mobility databases using the CALPHAD method. The present work reviews the development of CALPHAD thermodynamic and diffusion mobility databases and how these databases are used in various applications.

Thermodynamics

The calculation of phase equilibria uses the condition that the Gibbs energy at thermodynamic equilibrium is at a minimum for a given temperature, pressure and composition. Gibbs derived the well known equilibrium condition that the chemical potential μ_n^ϕ of each component n is the same in all phases ϕ

$$\mu_1^I = \mu_1^{II} = \dots = \mu_1^\phi \mu_2^I = \mu_2^{II} = \dots = \mu_2^\phi; \mu_n^I = \mu_n^{II} = \dots = \mu_n^\phi \quad (1)$$

The chemical potentials are related to the Gibbs energy by the well known equation

$$G = \sum_{i=1}^n \mu_i x_i \quad (2)$$

The description of the Gibbs energy of a system requires assignment of thermodynamic functions for each phase. These descriptions of the Gibbs energy can be used together with equation (1) in numerical calculations to minimise the Gibbs energy for prescribed conditions. All of the CALPHAD type software tools use methods like the two-step method of Hillert²⁴ or the one step method Lukas *et al.*²⁵ to minimise the Gibbs energy. The equations obtained from these methods are usually non-linear and can be solved numerically, for example using a Newton–Raphson technique.

Model descriptions

The CALPHAD method employs a variety of model functions to describe the temperature, pressure and concentration dependencies of the free energy functions of the various phases. The contributions to the Gibbs energy of a phase ϕ can be written

$$G^\phi = G_T^\phi + G_P^\phi + G_M^\phi \quad (3)$$

where G_T^ϕ is the contribution to the Gibbs energy from the temperature T and the composition x alone; G_P^ϕ is the contribution from the pressure P and G_M^ϕ is the magnetic contribution by the Curie or Néel temperature T_C and the average magnetic moment per atom β_0 . The latter two contributions can also depend on T and x .

The temperature dependence of the Gibbs energy of a pure substance is usually expressed as a power series of T

$$G = a + bT + cT \ln(T) + dT^2 + eT^3 + fT^{-1} + gT^7 + hT^{-9} \quad (4)$$

where a, \dots, h are coefficients.²⁶ This guarantees that the heat capacity C_P is represented as simple power series of T

$$C_P = -c - 2dT - 6eT^2 - 2fT^{-2} - 42gT^6 - 90hT^{-10} \quad (5)$$

These functions are valid for temperatures above the Debye temperature. In each of the equations in the following models, the coefficients of the functions describing the concentration dependence can have such a temperature dependence. Frequently only the first two terms of equation (4) are used for the representation of the excess Gibbs energy. Dinsdale²⁶ also gives expressions for the effects of pressure and magnetism on the Gibbs energy. However, the pressure dependence for condensed systems at normal pressures is usually ignored.

For multicomponent systems, it is useful to distinguish three contributions to the concentration dependence to the Gibbs energy of a phase G^ϕ

$$G^\phi = G^0 + G^{\text{ideal}} + G^{\text{xs}} \quad (6)$$

where G^0 corresponds to the Gibbs energy from the rule of mixture based on the mole fractions of the constituents of the phase, G^{ideal} corresponds to the entropy of mixing for an ideal solution and G^{xs} is the so

called excess term. For G^{xs} Hildebrand²⁷ introduced the term ‘regular solution’ to describe interactions of different elements in a random solution. However, many phases deviate from this ‘regularity’, i.e. show a stronger compositional variation in their thermodynamic properties, and other models are needed to describe the excess Gibbs energy. For example, to describe short range order in liquid phases a number of models have been proposed. Most commonly used are the ionic liquid model,^{28,29} the associate model³⁰ and the modified quasichemical model.^{31,32} For ordered solid phases, Wagner and Schottky³³ introduced the concept of defects on the crystal lattice to describe deviations from stoichiometry. Many other models also have been proposed. Today the most commonly used models for solid phases (listed in the order of increasing complexity) are those for stoichiometric phases, regular solution type models for disordered phases, and sublattice models for ordered phases having a range of solubility or exhibiting an order–disorder transformation.³⁴ The following examples give descriptions of models for binary phases, which can easily be expanded for ternary and higher order phases.

The Gibbs energy of a binary stoichiometric phase is given by

$$G^{\phi} = x_A G_A^0 + x_B G_B^0 + \Delta G^f \quad (7)$$

where x_A and x_B are mole fractions of elements A and B and are given by the stoichiometry of the compound, G_A^0 and G_B^0 are the respective reference states or lattice stabilities of elements A and B , and ΔG^f is the Gibbs energy of formation. The first two terms and the third term correspond to G^0 and G^{xs} in equation (6) respectively. G^{ideal} of equation (6) is zero for a stoichiometric phase since there is no random mixing.

Binary solution phases, such as liquid and disordered solid solutions, are described as random mixtures of the elements by a regular solution type model

$$G^{\phi} = x_A G_A^0 + x_B G_B^0 + RT(x_A \ln x_A + x_B \ln x_B) + x_A x_B \sum_{i=0}^n L_i (x_A - x_B)^i \quad (8)$$

where x_A , x_B , G_A^0 and G_B^0 are the same as equation (7), and R is the molar gas constant. The first two terms correspond to G^0 and the third term, from random mixing, corresponds to G^{ideal} in equation (6). The L_i of the fourth term are coefficients of the excess Gibbs energy term G^{xs} in equation (6). Equation (8) describes a regular solution when L_0 is the only excess energy contribution and has no temperature dependence. The sum of the terms $(x_A - x_B)^i$ is the so called Redlich–Kister polynomial.³⁵ This is the most commonly used polynomial in regular solution type descriptions. Although other polynomials²⁵ have been used in the past, in most cases they can be converted to Redlich–Kister polynomials.

The sublattice is a very general model which is frequently used to describe ordered binary solution phases. The basic premise for this model is that a sublattice is assigned for each distinct site, ideally a Wyckoff site, in the crystal structure. For example, the structure of the Laves phase Mg_2Cu (C15) consists of two sublattices, one of which is occupied predominantly by Mg atoms and the other by Cu atoms. An ordered

binary solution phase with two sublattices that exhibit substitutional deviation from stoichiometry can be described by the expression

$$G^{\phi} = y'_A y''_A G_{AA}^0 + y'_A y''_B G_{AB}^0 + y'_B y''_A G_{BA}^0 + y'_B y''_B G_{BB}^0 + RT[a'(y'_A \ln y'_A + y'_B \ln y'_B) + a''(y''_A \ln y''_A + y''_B \ln y''_B)] + y'_A y'_B y''_A \sum_{i=0}^{n_1} L_i^1 (y'_A - y'_B)^i + y'_A y'_B y''_B \sum_{i=0}^{n_2} L_i^2 (y'_A - y'_B)^i + y'_A y''_A y''_B \sum_{i=0}^{n_3} L_i^3 (y''_A - y''_B)^i + y'_B y''_A y''_B \sum_{i=0}^{n_4} L_i^4 (y''_A - y''_B)^i + y'_A y'_B y''_A y''_B L^5 \quad (9)$$

where y'_A, y'_B, y''_A and y''_B are the species concentrations of elements A and B on the two sublattices with $a'y'_A + a''y''_A = x_A$, $a'y'_B + a''y''_B = x_B$ and $y'_A + y'_B = 1$, $y''_A + y''_B = 1$. a' and a'' are the site fractions of the sublattices and are given by the number of sites in the unit cell, for example for Mg_2Cu the site fractions are $a^{Mg} = 0.667$ and $a^{Cu} = 0.333$. The first four terms of equation (9) describe the contributions from the Gibbs energies of the so called end member phases $G_{AA}^0, G_{AB}^0, G_{BA}^0$ and G_{BB}^0 . End member phases are formed when each sublattice is occupied only by one kind of species, which can be either real phases ($A'_A B'_B$ with A atoms on the first sublattice and B atoms on the second sublattice) or hypothetical phases ($A'_A A''_A, B'_A A''_A$ and $B'_B B''_B$). The Gibbs energy of an end member phase is similar to the Gibbs energy of a stoichiometric phase (equation (7)). The fifth term corresponds to G^{ideal} in equation (6) describing the contribution from mixing on each sublattice. The remaining terms are the excess Gibbs energy term G^{xs} in equation (6) and describe interactions between the atoms on one sublattice in a manner similar to regular solution type models for disordered solution phases. For any given temperature and composition the phase must also be in internal equilibrium, i.e.

$$\frac{\partial G^{\phi}}{\partial y'_k} = 0$$

The Gibbs energy minimisation for the internal equilibrium can be coupled with the Gibbs energy minimisation for the global equilibrium.²⁵

The sublattice model description (equation (9)), also called the compound energy formalism (CEF), was first introduced by Sundman and Ågren³⁶ and later refined by Andersson *et al.*³⁷ Ansara *et al.*³⁸ and Ferro and Cacciamani.³⁹ Ferro and Cacciamani³⁹ also discussed the criteria for determining the number of sublattices and their site fractions for a number of common ordered intermetallic structures.

The compound energy formalism can also be used to describe phases that exhibit order–disorder transformations. For example, Ansara *et al.*⁴⁰ derived a model description for the order–disorder transformation of fcc/L1₂. This model was later modified by Ansara *et al.*⁴¹ to allow independent evaluation of the thermodynamic properties of the ordered and disordered state. The Gibbs energy of such an order–disorder phase consists of three parts

$$G^\varphi = G^{\text{dis}}(x_i) + G^{\text{ord}}(y_i^l, x_i)$$

$$\text{with } G^{\text{ord}}(y_i^l, x_i) = G^{\text{ord}}(y_i^l) - G^{\text{ord}}(x_i) \quad (10)$$

where l is the sublattice index. $G^{\text{dis}}(x_i)$ is the Gibbs energy of the disordered state and has the same form as the Gibbs energy description of the substitutional solution phase (equation (8)). The term $G^{\text{ord}}(y_i^l, x_i)$ is the contribution from the sublattice model description as in equation (9) and is composed of two contributions. $G^{\text{ord}}(y_i^l)$ is the contribution of the ordered state and $G^{\text{ord}}(x_i)$ is the implicit Gibbs energy contribution of the sublattice model description to the disordered state. If the phase is completely disordered, i.e. $y_i^l = y_i^{l'} = \dots = x_i$, the contribution of the sublattice description is $G^{\text{ord}}(y_i^l) - G^{\text{ord}}(x_i) = 0$ and the disordered state is only described by $G^{\text{dis}}(x_i)$. Since G^{ord} must be at a minimum for $y_i^l = y_i^{l'} = \dots = x_i$, the relationship between concentration x_i and the site fractions y_i^l results in constraints for the coefficients in the sublattice model description. Ansara *et al.*⁴¹ and Kusoffsky *et al.*⁴² derived these constraints for A1/L1₂/L1₀ ordering in the fcc family and Dupin and Ansara⁴³ derived them for A2/B2 ordering in the bcc family. The constraints to treat the A3/D0₁₉/B19 ordering in the hcp family are the same as for the A1/L1₂/L1₀ ordering in the fcc family since the ordering in both cases involves four sublattices.⁴⁴

Other approaches to describe the energetics of order–disorder transitions use a cluster expansion Hamiltonian.^{45,46} The thermodynamic quantities and phase diagrams can be obtained from Monte Carlo (MC) simulations⁴⁶ or from the cluster variation method (CVM).⁴⁷ In CVM calculations, configurational entropy expressions are typically complex and the effective interaction ranges are short.⁴⁸ The complexity of the expression increases exponentially with cluster size and with the number of components; also, excessively large clusters are often necessary to include a sufficient set of effective interactions. Therefore, CVM has been used only to model binary and ternary systems that can be described with very short range interactions. Inden and Pitsch⁴⁹ and de Fontaine⁴⁷ gave extensive reviews of these calculations. Even for binary systems, setting up the calculation can be time consuming. Van de Walle *et al.*^{50,51} developed the alloy theoretic automated toolkit for such calculations. The alloy theoretic automated toolkit is a collection of several tools, including one to construct cluster expansion Hamiltonians from first principles calculations and a MC simulation code for obtaining thermodynamic quantities and phase diagrams. Oates *et al.*^{48,52} proposed the cluster site approximation to treat order–disorder transformations. The cluster site approximation clusters are only permitted to share corners and, therefore, only the cluster energies contribute to the energy equation and the entropy expression remains fairly simple, which allows implementation in CALPHAD type software. Cluster site approximation has been applied in calculations of A1/L1₀/L1₂ ordering in ternary and quaternary systems^{53,54} and A3/D0₁₉/B19 ordering in a binary system.⁵⁵ One advantage of the cluster based methods is that the effect of short range order is explicitly described. However, it is possible to take the effect of short range order into account with CEF.⁴⁴

Determination of coefficients

The coefficients of the Gibbs energy functions are determined from experimental data for each system.

To obtain an optimised set of coefficients, it is desirable to take into account all types of experimental data, e.g. phase diagram, chemical potential and enthalpy data. Experimental data can be supplemented by data obtained from predictions. The predictions can be made by semi-empirical approaches, such as the Miedema model,⁵⁶ embedded atom methods,⁵⁷ or first principles calculations using density functional theory (DFT) methods. Hafner *et al.*⁵⁸ gave an overview of a variety of DFT methods. Turchi *et al.*⁵⁹ also gave an overview and examine the links between these DFT methods, experiments and the CALPHAD method. Data from predictions, especially if the structure of the phase is considered, are very valuable if it is not possible to determine quantities experimentally, for example the Gibbs energy of formation of a hypothetical end member phase needed for a CEF model description.

The Gibbs energy coefficients of the model description can be determined from these data by a trial and error method or mathematical methods. The trial and error method is feasible only if a few different data types are available. This method becomes increasingly cumbersome as the number of components and/or number of data types increases. In this case mathematical methods, such as the least squares method of Gauss,⁶⁰ the Marquardt method⁶¹ or Bayesian estimation method,⁶² are more efficient. The determination of the coefficients is frequently called ‘assessment’ or ‘optimisation’ of a system. Lukas *et al.*⁶³ provide detailed guidance for the assessment procedure. The first step in the assessment of the thermodynamic description of a system is the critical evaluation of the available data, since an equally weighted use of all available data in most cases will result in a rather arbitrary description of the system. During the assessment the validity of the thermodynamic descriptions of the individual phases must be verified. The description must be able to produce the phase diagram without artefacts over a wide temperature and composition range as well as producing reasonable metastable phase diagrams where one or more phases are absent.⁶⁴

Higher component systems

A higher component system can be calculated from thermodynamic extrapolation of the thermodynamic excess quantities of the constituent subsystems. Several methods exist to determine the weighting terms used in such an extrapolation formula. Hillert⁶⁵ analysed various extrapolation methods and recommended the use of Muggianu’s method⁶⁶ since it can easily be generalised. The Gibbs energy of a ternary solution phase determined by extrapolation of the binary energies, described by Redlich–Kister polynomials, using Muggianu’s method is given by

$$G^\varphi = x_A G_A^0 + x_B G_B^0 + x_C G_C^0 + RT(x_A \ln x_A + x_B \ln x_B + x_C \ln x_C) + x_A x_B \sum_{i=0}^{n_{AB}} L_i^{AB} (x_A - x_B)^i + x_A x_C \sum_{i=0}^{n_{AC}} L_i^{AC} (x_A - x_C)^i + x_B x_C \sum_{i=0}^{n_{BC}} L_i^{BC} (x_B - x_C)^i \quad (11)$$

where the parameters, G_j^0 and L_i^{jk} , have the same values as in equation (8) for each of the binary systems. If

necessary, a ternary term, $x_A x_B x_C G^{ABC}(T, x_i)$, can be added to describe the contribution of three element interactions to the Gibbs energy.

The usual strategy for assessment of multicomponent systems is first to derive the thermodynamic descriptions of the constituent binary systems. Thermodynamic extrapolation methods are then used to extend the thermodynamic functions of the binaries into ternary and higher component systems. The results of such extrapolations can then be used to design critical experiments. The results of the experiments are then compared to the extrapolation and, if necessary, additional terms can be added to the excess Gibbs energies of the phases in the higher order system. As mentioned previously, the coefficients of the interaction functions are optimised on the basis of these data. In principle, this strategy is followed until all 2, 3, ... n constituent systems of an n component system have been assessed. However, experience has shown that, in most cases, no or very minor corrections are necessary for reasonable prediction of quaternary or higher component systems. Since true quaternary phases are rare in metallic systems, assessment of most of the ternary constituent systems is often sufficient to describe an n component system.

The initial results from the extrapolation of the higher component system provide an additional criterion for the quality of the descriptions of the subsystems. If the result of extrapolation contradicts the experimental observations, it may become necessary to reassess the description of one of the subsystems.⁶⁴ A phase that does not occur in all of the subsystems but has a homogeneity range in the higher component system may require that it is modelled as a metastable phase in the subsystems in which it does not occur. It is pertinent for the extrapolation of higher component systems that not only the models but also the lattice stabilities and the Gibbs energies of the end member phases of the subsystem descriptions are compatible. Therefore, it is not advisable to determine these quantities from the assessment of the higher component system. It is preferable to obtain these quantities from first principles methods or use estimates if first principles data are not available. Dinsdale²⁶ gives the lattice stabilities of the elements in their stable structures and for the close packed structures fcc, bcc and hcp. Sluiter⁶⁷ used DFT to calculate the structural enthalpy differences for the pure elements at 0 K for cubic prototype structures of the elements and a series of topologically close packed structures.

Software tools and databases

A variety of software packages can be used for the calculation of phase diagrams. Some of these software packages are only available for windows operating systems while others are also available for Linux systems. General, fully integrated software packages, such as FactSage,⁶⁸ (Commercial products are referenced in the present paper as examples. Such identification does not imply recommendation or endorsement by the National Institute of Standards and Technology) MTDATA,⁶⁹ PANDAT⁷⁰ or Thermo-Calc,⁷¹ offer great versatility with a suite of modules for data input, different types of calculations and graphical output of the results. Most of the model descriptions used for alloy and ceramic systems are common to all these programs.

However, not every package has other specific model descriptions, for example, the quasichemical model or models for aqueous and polymer solutions. Some versions of the software provide user friendly graphic user interfaces. A general calculation module allows the user to specify the equilibrium conditions for the calculation while other modules offer predefined types of calculations. Although the features offered by the individual software packages differ, some modules, such as for the calculation of binary and ternary phase diagrams, are common to all software packages. The software packages allow a choice of thermodynamic databases, including user specified databases. Some of the software packages also include an assessment module for the refinement of the thermodynamic functions of the phases with respect to experimental data; this is a valuable tool for the development of thermodynamic databases. In addition, the software packages provide code libraries that can be linked with user written applications.

The software modules of other packages, e.g. MALT,⁷² its successor MALT2⁷³ and ThermoSuite,⁷⁴ are designed to calculate specific equilibria. These packages are coupled with their own databases, but also allow user supplied databases. The HSC package⁷⁵ offers a wide variety of equilibrium calculations and includes modules for process simulations. However, the calculations are limited to condensed stoichiometric compounds and gaseous species. Another group of calculation tools are task specific tools, such as JMatPro⁷⁶ or SolCalc.⁷⁷ Both tools perform solidification specific calculations. In addition, JMatPro can also calculate various mechanical, thermophysical and physical properties and phase transformation diagrams.⁷⁸

Over time, a large number of thermodynamic databases have become available. These databases have been constructed from the assessments of binary, ternary and quaternary systems. For the description of commercial alloys, it is quite likely that at least a dozen elements need to be considered. The number of constituent subsystems of an n component system is determined by the binomial coefficient $\binom{n}{k}$, where k is the number of components in the subsystem. A 12-component system consists accordingly of 66 binary, 220 ternary and 495 quaternary subsystems. These numbers suggest that it is impossible to obtain descriptions of all the subsystems in a reasonable time frame. However, as mentioned previously, only rarely are quaternary excess parameters needed. If the database is for base element X, it is sufficient to consider only the X based ternary systems, considerably reducing the number of needed assessments. Also, if more than one element occurs only in fairly small quantities in the alloy family of interest then assessments of binary systems containing only these elements or ternary systems with two or three of these elements are generally not very important for obtaining correct predictions. Based on this, a number of databases have been developed for various commercial alloy systems and inorganic systems. However, because software packages assume different computer file formats for the databases, attention must be paid to insure compatibility between database file format and program package before databases are acquired.

One of the most general databases is the SGTE Solution Database,⁷⁹ SSOL. This database contains data

for the liquid phase and numerous crystalline phases in >400 binary, ternary and quaternary alloy systems. Specialty databases for alloys usually focus on one base element while those for inorganic systems may focus on a substance class or manufacturing application. These databases are under constant development and new databases are in the process of being developed. The most up to date information can be found on the websites of the individual database developers: CompuTherm LLC,⁸⁰ FACT/CRCT,⁸¹ Materials Design Technology,⁸² MTDATA,⁸³ NIST,⁸⁴ ThermoCalc,⁸⁵ Thermotech⁷⁸ and others. Other specialty databases, such as those resulting from the COST 507⁸⁶ and COST 531⁸⁷ actions of the European Union, although published, may not be widely available in electronic format. Pure substance databases, such as the SGTE Pure Substance Database,⁷⁹ SSUB, the FACT General Compound Database,⁸¹ FACT53, or the HSC Chemical Database,⁷⁵ contain a large number of Gibbs energy functions for stoichiometric compounds and gaseous species and, therefore, also have a wide array of applications. These databases are frequently used in conjunction with other databases. If data from different databases are merged it is important that the reference states used for the thermodynamic descriptions in these databases are compatible or erroneous results will be obtained.

Diffusion

The interdiffusion between two materials is described by a flux equation (Fick's law) and the continuity equation^{88,89}

$$J_i = -D_i \frac{\partial c_i}{\partial z} \quad (12)$$

$$\frac{\partial c_i}{\partial t} = \frac{\partial}{\partial z} \left(D_i \frac{\partial c_i}{\partial z} \right) \quad (13)$$

where z is the diffusion distance and J_i describes the amount of material that passes through a unit area of a plane per unit time t within a volume fixed frame of reference (otherwise known as the interdiffusion flux). The variable c_i is the concentration of component i (note: $c_i = x_i V_m$ where V_m is the molar volume of the phase) and D_i is the diffusivity of component i , which is concentration and temperature dependent. Onsager^{90,91} was the first to extend Fick's law to multicomponent alloys when he postulated that the thermodynamic flux was linearly related to the composition gradient. It is these Onsager relationships that have been employed by Ågren and co-workers¹⁸⁻²⁰ to implement the CALPHAD method for the development of diffusion mobility databases. Recent reviews of diffusion in materials are given by Philibert⁹² and Koiwa.⁹³

Diffusion data

A variety of different types of diffusion data can be used to evaluate diffusion mobility functions, including diffusion coefficients, composition profiles and layer growth widths. Tracer, intrinsic and chemical diffusivities can all be extracted from various types of diffusion experiments. In the present paper, the diffusion definitions used are those defined by the International Union of Pure and Applied Chemistry recommendations of 1999.⁹⁴ Tracer diffusion is the migration of a tagged

atom through a material of which it is a component. As such, the tracer diffusivity is generally measured by introducing a radioactive isotope in dilute concentration into an otherwise homogeneous material. Thus, the only driving force in the system is that of the concentration gradient of the tracer. In a homogenous material the mean square displacement of the tracer in the z direction is defined by the Einstein formula for Brownian motion (random walk) as

$$\langle z_i^2 \rangle = 2D_i^* t \text{ where } D_i^* = RTM_i \quad (14)$$

where D_i^* is the tracer diffusion coefficient, t is the diffusion time and M_i is the atomic mobility of the i atoms. The tracer diffusion coefficient is equal to the self-diffusion coefficient D_i^S , if diffusion takes place by uncorrelated atomic jumps, otherwise the tracer diffusion coefficient is related to the self-diffusion coefficient by the correlation factor f , $D_i^* = fD_i^S$. The correlation factor is dependent on the crystal structure and introduces off diagonal terms into the M_i matrix. For the bcc and fcc crystal structures assuming a vacancy diffusion mechanism, the contribution of these off diagonal terms is small. Thus, for simplicity, these terms are not included in the present discussion; however, calculation methods are discussed by Philibert⁹⁵ and Shewmon.⁹⁶ The intrinsic diffusion coefficient defines the non-reciprocal atomic flux and is measured with inert markers (Kirkendall markers).^{97,98} The intrinsic diffusivity is the product of the diffusion mobility and the thermodynamic factor in the lattice fixed frame of reference.

$$D_{kj}^L = x_k M_k \frac{\partial \mu_k}{\partial x_j} \quad (15)$$

The component j is the diffusing component and k is the gradient component. The partial derivative of the chemical potential μ_k with respect to the mole fraction x_j corresponds to the thermodynamic factor.⁹⁹ Note that the partial derivative of the chemical potential can be easily calculated using an appropriate multicomponent thermodynamic database. However, the thermodynamic factor must be evaluated in the form $\mu_k(x_1, x_2, \dots, x_n)$ as there are $n-1$ independent concentrations.

The chemical diffusion coefficient D_{kj}^V is a measure of the diffusivity of one component in the presence of a gradient in chemical potential measured in the volume fixed frame of reference

$$D_{kj}^V = \sum_{i=1}^n (\delta_{ik} - x_k) x_i M_i \frac{\partial \mu_i}{\partial x_j} V_m \quad (16)$$

The δ_{ik} is the Kronecker delta symbol and equals one when $i=k$ and zero when $i \neq k$. As there are only $(n-1)$ independent components, diffusion couple experiments are only able to directly evaluate the interdiffusion coefficient \tilde{D}_{kj}^n

$$\tilde{D}_{kj}^n = D_{kj}^V - D_{kn}^V \quad (17)$$

where n is the dependent variable. While interdiffusion coefficients are the most commonly reported diffusion measurements, there are several error sources associated with these measurements. The Boltzmann–Matano method^{100,101} is often used to determine the binary interdiffusion coefficient from measured composition

profiles. However, this method does not consider any change in molar volume across the diffusion couple. When significant molar volume changes are present, the interdiffusion coefficients should be calculated using methods that include the composition dependence of the molar volume, such as the Sauer–Friese method¹⁰² as adopted by Wagner.¹⁰³

As the number of elements in the diffusion couples increases, determining the interdiffusion coefficients becomes more difficult; for each interdiffusion coefficient, $(n-1)$ composition profiles with different terminal compositions must intersect at one common intersection point. In an effort to overcome this complexity, Dayananda and Sohn¹⁰⁴ derived a new analysis method that enables the determination of an average interdiffusion coefficient over a selected composition range from a single multicomponent diffusion couple by integrating the interdiffusion flux of a component over the diffusion distance for a selected range of compositions. This method has been implemented in the computational software program, MultiDiFlux.¹⁰⁵

In addition to the variety of experimental data available for diffusion mobility assessments, first principles calculations may be available to help estimate difficult to measure or metastable diffusion coefficients. Janotti *et al.*^{106,107} used density functional equations in the local density approximation to calculate self-activation energies for transition metals in nickel and demonstrated that first principles calculations can be used to predict systematic trends in diffusion rates as a function of atomic number. Mishin and co-workers have used embedded atom potentials to evaluate diffusion mechanisms and determine activation energies for a variety of systems, including Ni–Al,^{108,109} Ti–Al^{110,111} and Fe on a Fe(001) surface.¹¹² Kinetic Monte Carlo simulations using Kub-Green expressions to extract diffusion coefficients have been used by van der Ven and co-workers to predict diffusion coefficients in model binary substitutional alloys.^{113,114}

Descriptions and models

As multicomponent diffusion coefficients may be strongly dependent on composition and experimental measurements of all the needed higher order diffusion coefficients in a multidimensional composition and temperature space are impractical, Andersson and Ågren²⁰ developed a formalism based on the CALPHAD method to describe diffusion mobilities in multicomponent systems. These diffusion mobilities can then be combined with the needed thermodynamic factors to calculate the multicomponent diffusion coefficients.

Disordered phases

Assuming a vacancy exchange diffusion mechanism in a crystalline phase, the mobility matrix M_i which is both composition and temperature dependent, can be written as

$$M_i = \Theta_i \frac{1}{RT} \exp\left(\frac{\Delta Q_i^*}{RT}\right) \quad (18)$$

Following the work of Andersson and Ågren,²⁰ the off diagonal terms of the diffusion mobility matrix are assumed to be zero, i.e. as for the disordered phases, correlation effects are assumed to be negligible. M_i is the

mobility of component i in a given phase, Θ_i ($\text{m}^2 \text{s}^{-1}$) represents the effects of the atomic jump distance (squared) and the jump frequency, ΔQ_i^* (J mol^{-1}), is the diffusion activation energy of component i in a given phase. Ågren and co-workers^{20–23,115,116} assumed constant partial molar volumes and expressed the composition and temperature dependence of each ΔQ_i^* in terms of a Redlich–Kister³⁵ polynomial

$$\Delta Q_i^* = \sum_j x_j Q_i^j + \sum_p \sum_{j>p} x_p x_j \sum_k {}^k A_i^{pj} (x_p - x_j)^k \quad (19)$$

where the Q_i^j and the ${}^k A_i^{pj}$ are linear functions of temperature. The expansion of the composition dependence in terms of a Redlich–Kister polynomial is similar to the CALPHAD method^{15,16,63} used in the development of the thermodynamic databases (equation (11)). Note that for a given diffusing component i , if all Q_i^j are equal and ${}^k A_i^{pj}$ equals zero, then ΔQ_i^* and the corresponding M_i are not concentration dependent. The composition dependence of Θ_i can also be represented by equation (19); however, it is frequently assumed that M_i^0 depends exponentially on composition¹¹⁷ and is included in the activation energy term

$$\Delta Q'_i = \Delta Q_i - RT \ln M_i^0 \quad (20)$$

Interstitial diffusion

Interstitial elements can be added to the database using a sublattice description and by assuming the partial molar volume of the interstitial element is zero.¹⁸ An example of this model is the addition of carbon to the Fe–Ni–Cr fcc phase diffusion assessment by Jönsson.¹¹⁸

Magnetic transition

For the substitutional elements, such as transition metals, Jönsson^{119,120} modelled the effect of the transition between the para- and ferromagnetic states on the diffusion in bcc alloys. Jönsson showed that the effect of magnetic ordering on diffusion can be included using the model of Braun and Feller-Kniepmeier,¹²¹ which relates the change in diffusivity to the magnetic enthalpy. For interstitial elements, such as C or N, the effect of the magnetic transition is less well established. The magnetic transition has a strong effect on carbon diffusivity¹²² to which Ågren¹²³ applied a formalism in which the same activation energy is applied for both the paramagnetic and ferromagnetic states. However, no significant change in the nitrogen diffusivity is observed as the magnetic transition occurs.

Ordered phases

For an ordered phase, the composition dependence of the diffusion mobilities must include the effect of chemical ordering. Based on the model by Girifalco,¹²⁴ which assumes the activation energy from chemical ordering is dependent on a long range order parameter, Helander and Ågren¹¹⁵ suggested incorporating the effect of chemical ordering by dividing the activation energy into two terms:

- (i) the contribution from the disordered state ΔQ_k^{dis}
- (ii) the contribution from the ordered state ΔQ_k^{ord}

$$\Delta Q_k = \Delta Q_k^{\text{dis}} + \Delta Q_k^{\text{ord}} \quad (21)$$

where ΔQ_k^{ord} is defined as

$$\Delta Q_k^{\text{ord}} = \sum_i \sum_{j \neq i} \Delta Q_{kij}^{\text{ord}} (y'_i y''_j - x_i x_j) \quad (22)$$

and $\Delta Q_{kij}^{\text{ord}}$ are the contributions to the activation energy for component k as a result of the chemical ordering of the i and j atoms on the two sublattices; x_i is the mole fraction of component i ; and y'_i and y''_i the site fractions of component i on the given sublattices, as defined in equation (8). In the Helander and Ågren model the site fraction variable is used in place of the ordering variable used by Girifalco.

The Girifalco approach used by Helander and Ågren was developed for an AB (B2) alloy where diffusion occurs via jumps between two metal sublattices. However, Tókei *et al.*¹²⁵ verified that the Girifalco approach was also valid for A_3B (Fe_3Al) alloys ($D0_3$ ordering), where diffusion occurs via a network of nearest neighbour jumps. Thus, the phenomenological model developed by Helander and Ågren for the B2 phase should also be valid for other ordered phases, such as the γ' (Ni_3Al-L1_2) phase. This model for describing diffusion in ordered phases has been used successfully by Helander and Ågren¹¹⁶ to describe the Fe–Ni–Al diffusion in the B2 phase and by Campbell¹²⁶ to describe the Ni–Al–Cr diffusion in the B2 and γ' phases. An extension of this type of modelling in ordered phases is also being developed for oxide phases.¹²⁷

Stoichiometric phases

For binary stoichiometric phases the diffusivity is assumed to be proportional to the difference in the chemical potentials at each end of the stoichiometric phase multiplied by the mobility for the component in the phase.¹²⁸ Tracer diffusivity data for the component in the stoichiometric phase are used to assess the diffusion mobility functions. This type of model has been applied to the diffusivity of carbon in cementite.¹²⁹

Determination of diffusion mobility coefficients

Similar to the Gibbs energy function coefficients, the diffusion mobility coefficients in equations (19) and (22) are determined from experimental data for each system and can be evaluated using trial and error methods or mathematical methods that minimise the error between the calculated and experimental diffusion coefficients, as shown in Fig. 1. The PARROT optimiser¹³⁰ within the DICTRA code^{71,131} allows direct optimisation of diffusion mobility functions using a least squares error method. The assessment of the higher order components of the diffusion mobility functions follows the same procedure as described for the Gibbs energy functions.

The coefficients for diffusion mobility functions can be optimised using all of the diffusion data types described in the section on 'Diffusion data'. Tracer diffusivity data, which are independent of the thermodynamic factor, are the preferred data for assessments. However, the probability of being able to construct an entire multicomponent diffusion database only with available tracer diffusivity data is small. While both the intrinsic and interdiffusion coefficient data depend on thermodynamic quantities and require a thermodynamic database to be specified to complete the diffusion mobility assessment, Campbell *et al.*¹³² showed that

the difference between diffusion coefficients calculated with two different thermodynamic databases is within the experimental error when consistent thermodynamic descriptions were used. However, it is essential that both the thermodynamics and diffusion mobilities use the same model description for the concentration dependence of a given phase.

In addition to optimising the mobility functions using various composition dependent diffusion coefficient data, methods have been developed to optimise the diffusion mobility functions directly from experimental composition profiles. Both Campbell¹³³ and Höglund¹³⁴ have developed methods that combine DICTRA with an optimisation tool (MatLab or Mathematica) to assess the mobility parameters from experimental composition profiles. For a given set of mobility parameters, the difference between the experimental composition and calculated composition is defined by a least squares error function. The mobility parameters are optimised to minimise the error. This method has been successfully demonstrated for binary and ternary systems. Methods are currently being developed to use this type of approach to evaluate higher order systems.

The assessment may be evaluated by comparing calculations of multicomponent diffusion coefficients with experimental measurements not considered in the assessment. The assessed parameters may also be evaluated by comparing activation energies with diffusion correlations published in the literature¹³⁵ or with first principles calculations. A final test of the assessment may be the comparison of calculated and experimental composition profiles for various diffusion couples.

The current approach to modelling the diffusion coefficients provides an efficient representation of the composition dependence in multicomponent systems. The reduced number of parameters needed to describe diffusion in a multicomponent system occurs as a result of the assumption that the correlation factors are negligible in the lattice fixed frame of reference and only the diagonal terms of the mobility matrix must be evaluated. However, if the vacancy concentration is not in local equilibrium, the off diagonal terms resulting from the correlation factors should be considered.^{95,136} Using the CALPHAD method to describe the composition dependence of the mobility terms requires the determination of mobilities for fictive metastable end member phases. Examples of such quantities are the mobility of W in fcc W and the mobility of W in fcc Al at temperatures of above the fcc Al melting temperature (e.g. 1300°C). Determination of these end member quantities may follow approaches similar to those used to determine the lattice stabilities of the metastable thermodynamic quantities of the elements.^{15,16,63} This determination of diffusion activation energies for fictive end member phases may appear to limit the CALPHAD method. However, it is these determinations that enable the extrapolation to higher order systems where diffusion data are limited.

Databases and software tools

Until recently, the availability of multicomponent diffusion mobility databases has been limited. The largest and most general diffusion database is MOB2,⁸⁵ developed by Thermo-Calc AB. MOB2 was developed primarily for Fe based alloys but may be used for some other alloy systems depending on the

compositions of interest. MOB2 contains 75 elements and includes self-diffusion data for the bcc, fcc, hcp, cementite, Fe₄N and liquid phases. In addition to the self-diffusion data, the MOB2 database contains 10 binary, three ternary, one quaternary and one quinary assessments. The model by Jönsson¹¹⁹ for the ferromagnetic transition for the bcc Fe is also included. Liquid diffusion is modelled using a dilute approximation and assuming all the diffusivities are equal to $1 \times 10^{-9} \text{ m s}^{-2}$. A diffusion mobility database for the disordered Ni rich fcc phase was published by Campbell *et al.*^{132,137} This Ni mobility database contains 13 elements and includes 22 binary assessments, three ternary assessments and one quaternary assessment. An Al diffusion mobility, MOBAL⁸⁵ includes the assessment of the impurity diffusion data for 41 elements, liquid diffusivity data for 14 elements, and the binary assessment of the Al–Si system. Additional diffusion mobility descriptions for some fcc Co based alloys have been developed by Gómez-Acebo *et al.*¹³⁸ While the development of steel, superalloy, Al alloy, Zr based alloy,¹³⁹ cemented carbides^{140,141} and solder^{142,143} diffusion mobility databases continues, new databases for additional alloys systems are constantly being developed. As the number of diffusion mobility assessments continues to grow, it is important that the values of the self-activation energies are consistent so that binary and ternary assessments can be combined to build multicomponent databases.

The diffusion mobility databases are used to simulate diffusion processes in conjunction with a variety of computational tools, including finite difference codes that assume local equilibrium at each grid point (e.g. DICTRA), random walk methods¹⁴⁴ and phase field codes. The advantages and disadvantages of these different approaches have been reviewed by Strandlund and Larsson.¹⁴⁵ The phase field and random walk methods are more easily adapted to 2D and 3D calculations; however, these methods require significantly more computational time. Phase field simulations, which assume a dispersed interface, have been applied to a variety of systems including Ni base superalloys,^{146–149} steels,^{145,150} Ti–Al–V,¹⁵¹ and sintering of cemented carbides.¹⁵² Kirkendall porosity predictions in the Ni–Al–Cr system¹⁴⁴ and uphill diffusion predictions in the Fe–Si–C system¹⁴⁵ have been simulated using a random walk method.

When only the composition profiles are needed within a single phase region at a constant temperature, the Profiler code¹⁵³ may be used. It can be used to calculate diffusion profiles in for multicomponent systems ($n \leq 8$) by evaluating either a diffusivity or a square root diffusivity matrix¹⁵⁴ and then calculating a numerical solution for the linearised 1D form of equation (13).

Applications

In recent years the application of phase diagram and diffusion information obtained from calculations to practical processes has increased significantly. A variety of examples of applications are presented by Kattner *et al.*¹⁵⁵ and Ågren *et al.*¹⁵⁶ Extensive collections of detailed examples can be found in a number of books, such as ‘User applications of alloy phase diagrams’,¹⁵⁷ ‘User aspects of phase diagrams’,¹⁵⁸ or ‘The SGTE casebook, thermodynamics at work’.¹⁵⁹ A few examples

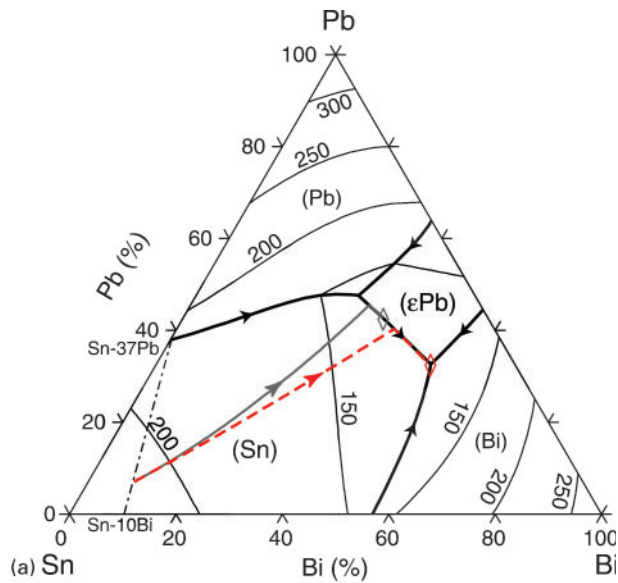
of the most common applications will be given here, as well as a few examples for selected special applications.

Phase equilibria calculations

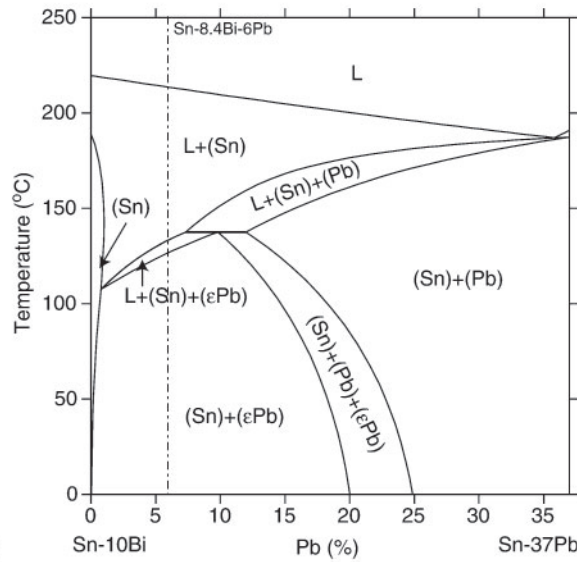
The most common and most general application of phase equilibria calculation is the generation of phase diagrams. A calculated binary phase diagram does not provide much more information than an experimentally obtained diagram, except that the calculated phase boundaries are consistent with the thermochemical properties of the individual phases. Ternary systems at constant pressure are usually represented by a series of projections and sections. Common graphic representations of a ternary system include the liquidus projection, isothermal sections and isopleths, each of which has its own advantages and disadvantages. For example, an isothermal section provides not only quantitative information of the phase boundaries, but also tie line and phase fraction information. It lacks, however, information about changing phase relationships as a function of temperature, information that can be provided by an isopleth, a T – x diagram where the concentration of one component or a concentration ratio is kept constant. However, tie lines rarely coincide with the plane of the isopleth and, therefore, no tie line or phase fraction information can be obtained from such a diagram. Since the thermodynamic description describes the entire system, the calculation can be used to generate sections and/or projections that provide the pertinent information for the task at hand.

Other important types of calculations, especially for systems with a large number of components, are based on stepping calculations. In 1D stepping calculations, one of the variables that was fixed for a single point equilibrium calculation (e.g. temperature) is stepped. At each step a single point equilibrium calculation is carried out. The graphical representation of the results is not a phase diagram but a property diagram displaying phase fractions, phase compositions and enthalpies, etc. as a function of the step variable. A well known example of this kind of calculation is the lever rule calculation of equilibrium solidification. However, stepping calculations can be used for many other applications by using another variable for stepping, such as the concentration or activity (partial pressure) of a component or the overall pressure. Other types of apparent stepping calculations are actually single equilibrium calculations that are connected by special conditions. Examples are the solidification calculation of the Scheil path or solidification calculation incorporating diffusion in the solid phase. The special conditions for the Scheil path calculation are derived from the assumptions of local equilibrium existing between the (uniform) liquid and the increment of solid formed at each temperature step, and that no diffusion occurs in the solid phase. This assumption produces the worst case of microsegregation with the lowest final freezing temperature.

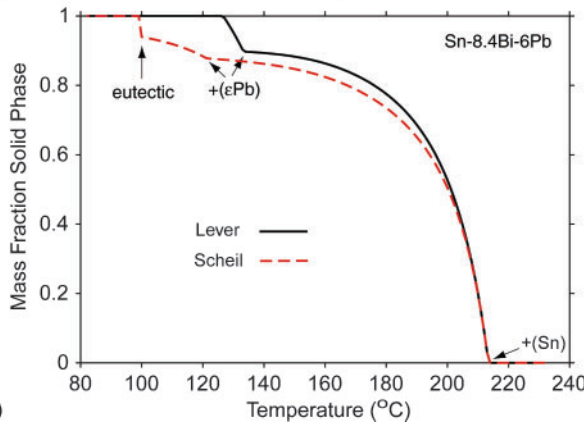
The use of different calculations and diagrams will be illustrated for the evaluation of a solder alloy. Liquidus temperature and freezing range are important properties for determining the suitability of a solder alloy candidate. However, the use of alloys for the pretinning of component leads and copper circuit board interconnects with a composition that is different from the alloy used for soldering may result in degraded properties of the solder joints, for example in a lower solidus



(a) Sn Bi Pb

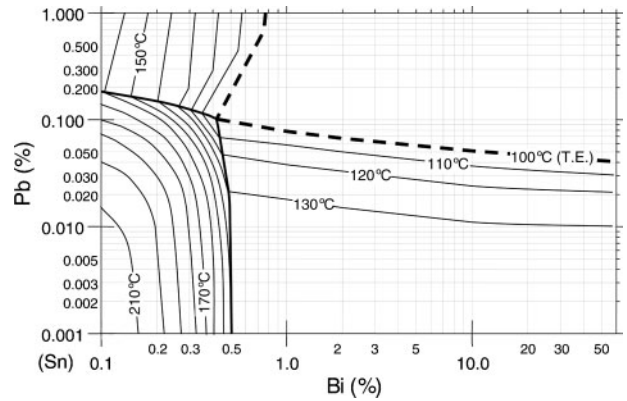


(b) Sn-10Bi Pb (%) Sn-37Pb



(c) Mass Fraction Solid Phase Temperature (°C)

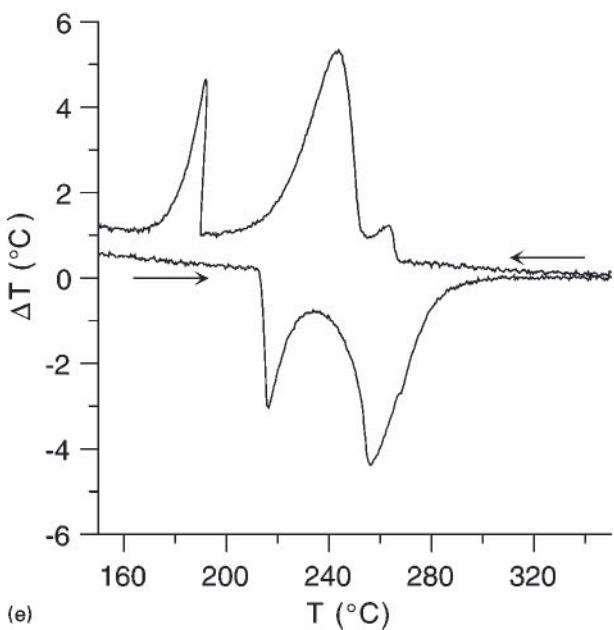
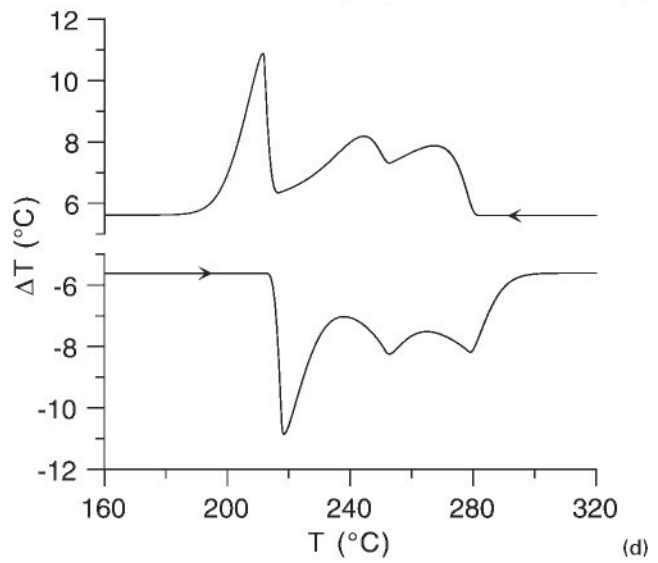
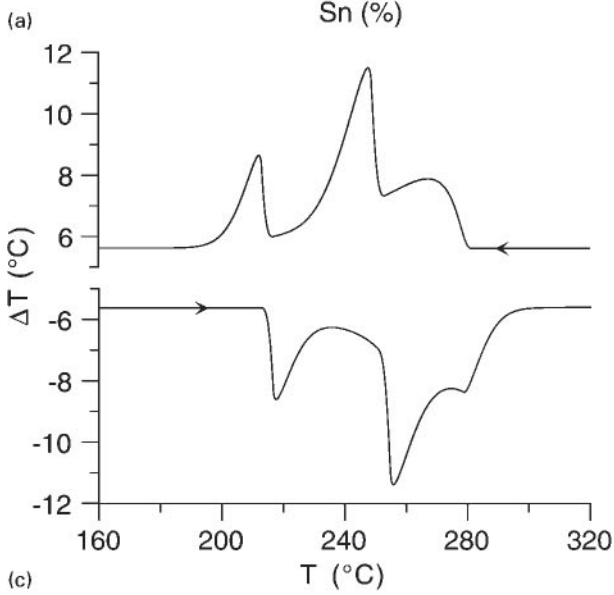
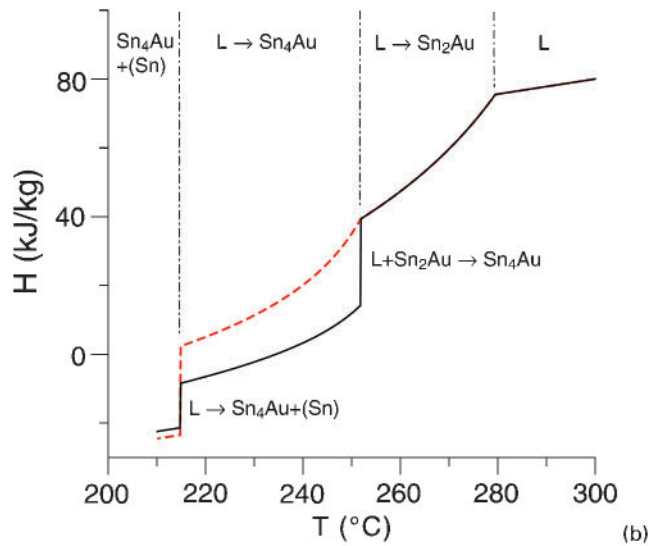
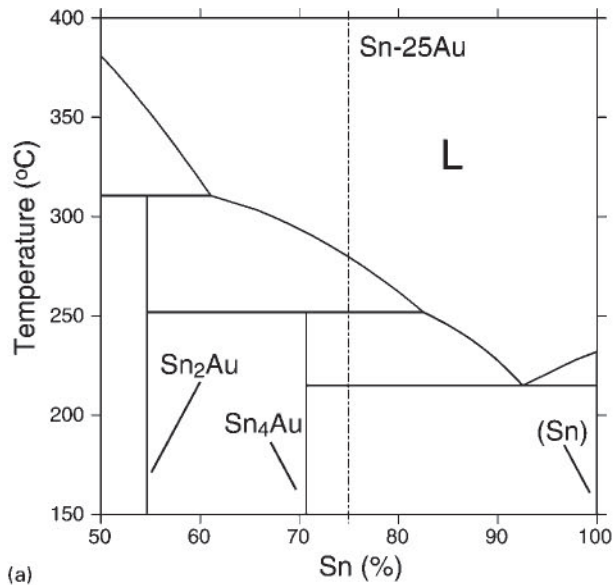
2 Calculation of Sn-Bi-Pb system: *a* projection of liquidus surface with lever rule (solid) and Scheil (dashed) paths (end points are marked by \diamond) of Sn-8.4Bi-6Pb alloy, section Sn-10Bi-Sn-37Pb is indicated by dot dashed line; *b* isopleth of section Sn-10Bi and Sn-37Pb, composition Sn-8.4Bi-6Pb is indicated by chain dotted line; *c* temperature phase fraction diagrams for lever rule and Scheil solidification of Sn-8.4Bi-6Pb alloy



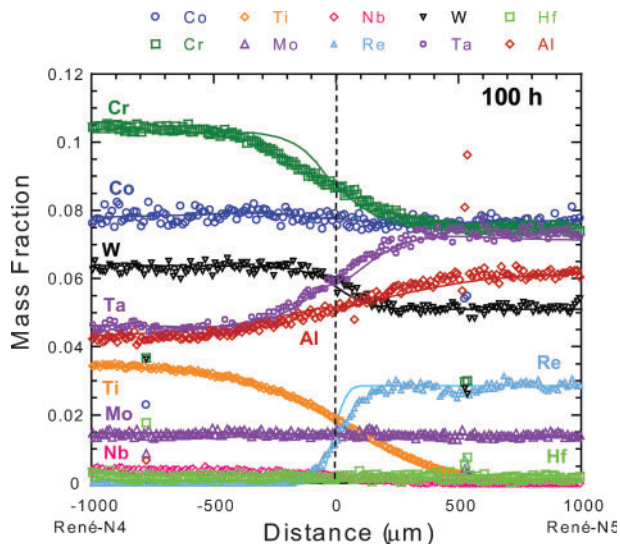
3 Calculated final freezing temperatures for Sn-Bi-Pb alloys using Scheil assumption

temperature. The Pb contamination of Sn-Bi solders was studied in detail by Moon *et al.*¹⁶⁰ using experimental methods in conjunction with calculations of the equilibrium phase diagram and Scheil solidification. The thermodynamic description from Yoon and Lee¹⁶¹ was used for the calculations. They found that a small amount of contamination by Pb results in the formation of a low melting eutectic at 100°C. The calculated projection of the liquidus surface, the isopleth of the section Sn-10Bi and Sn-37Pb (Bi and Pb concentrations are given as a percentage which represents a mass fraction with the balance being Sn) and the temperature phase fraction diagrams for lever rule and Scheil solidification for a Sn-8.4Bi-6Pb alloy are shown in Fig. 2. It is not possible to obtain the final freezing temperatures from the liquidus projection (Fig. 2a), although the diagram indicates the potential for the formation of the low melting eutectic if freezing following the Scheil path should occur. The isopleth (Fig. 2b) gives liquidus and solidus temperatures for lever rule solidification and shows the change in these temperatures with various levels of contamination of a Sn-10Bi solder with Sn-37Pb. The phase fraction diagram (Fig. 2c) shows that solidification following the lever rule is complete at 134°C, while Scheil solidification results in the formation of low melting eutectic at 100°C. The predictions from the Scheil path calculations were in accord with the experimental observations by Moon *et al.* A series of Scheil calculations was used by Moon *et al.* to map the final freezing temperatures of Pb contaminated Sn-Bi solders (Fig. 3) and showed that Pb contamination results in a significant decrease of the final freezing temperature, which is unacceptable for reliable solder joints.

One major advantage of the calculation of phase equilibria is that the results can easily be fed into other applications, either using look-up tables or direct coupling of the software using a programming interface. Boettinger and Kattner¹⁶² developed a heat flow model to simulate the response of a differential thermal analysis (DTA) apparatus for alloy melting and freezing. The program for the heat flow model uses a table with temperature and alloy enthalpy as input. The effect of the solidification behaviour of a Sn-25Au alloy on the DTA curve is illustrated in Fig. 4. The description from Liu *et al.*¹⁶³ was used for the calculations. The Sn rich part of the Sn-Au system (Fig. 4a) has a peritectic ($L + Sn_2Au \rightarrow Sn_4Au$) and a eutectic reaction



4 a Sn rich part of Sn–Au phase diagram, dot dashed line identifies Sn–25Au alloy, b enthalpy as function of temperature for lever rule (solid) and Scheil solidification (dashed) of Sn–25Au alloy; computed DTA curves for c lever rule condition, d Scheil condition and e measured curves



5 Calculated (solid lines) and experimental (symbols) compositional profiles for René-N4/René-N5 diffusion couples after 100 h at 1293°C

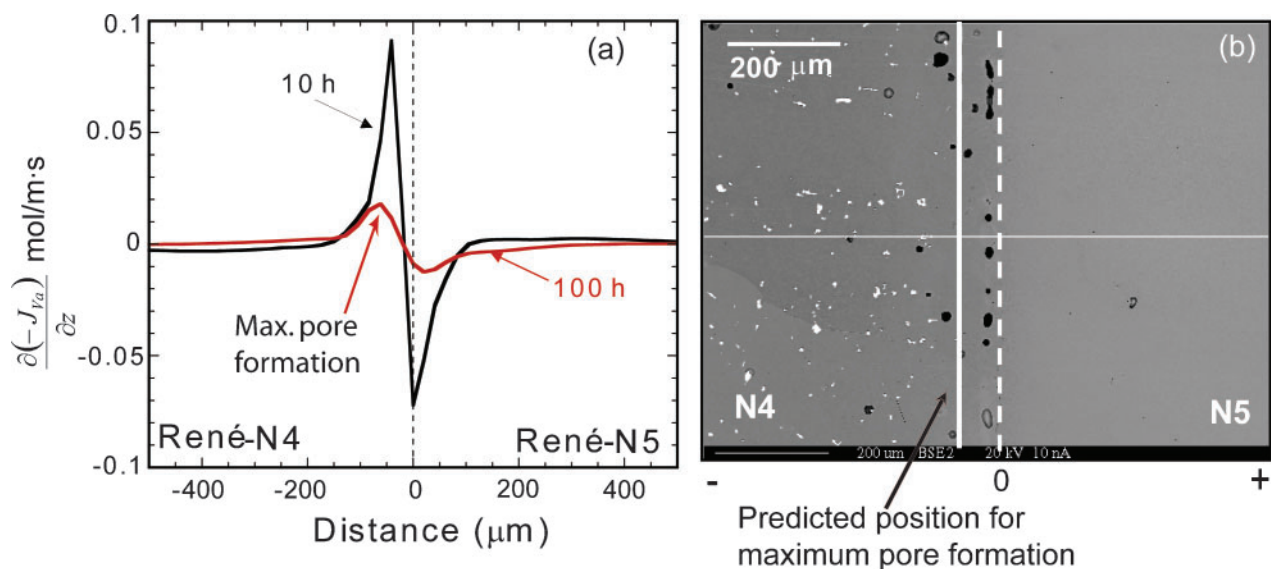
($L \rightarrow \text{Sn}_4\text{Au} + \text{Sn}$). Equilibrium (lever rule) solidification of the alloy results in two isothermal jumps in the enthalpy, as the peritectic and eutectic reactions occur (Fig. 4*b*). In the case of Scheil solidification the freezing process only switches from $L \rightarrow \text{Sn}_2\text{Au}$ to $L \rightarrow \text{Sn}_4\text{Au}$ and no isothermal jump of the enthalpy occurs at the peritectic temperature. When the alloy is heated and melting occurs the process is simply reversed. The simulated DTA curves are shown in Fig. 4*c* and *d*. The peak signal for the peritectic reaction during Scheil solidification is reduced and is less sharper compared to that of the lever rule solidification. It can also be seen that curves on heating and cooling do not mirror each other because of the thermal lag in the (simulated) apparatus. The simulated DTA signals compare well with the experimental results of a Sn–25Au alloy, as shown in Fig. 4*e*. The program was used by Boettinger *et al.*¹⁶⁴ to simulate DTA curves for various phase

diagram features and alloy freezing and melting conditions to obtain better understanding of the DTA response and to recommend guidelines for the analysis of curves from DTA and heat flux differential scanning calorimetry measurements. Other examples for using the output from phase equilibria calculations are the calculation of surface tension^{165,166} and viscosity of the liquid phase.¹⁶⁵

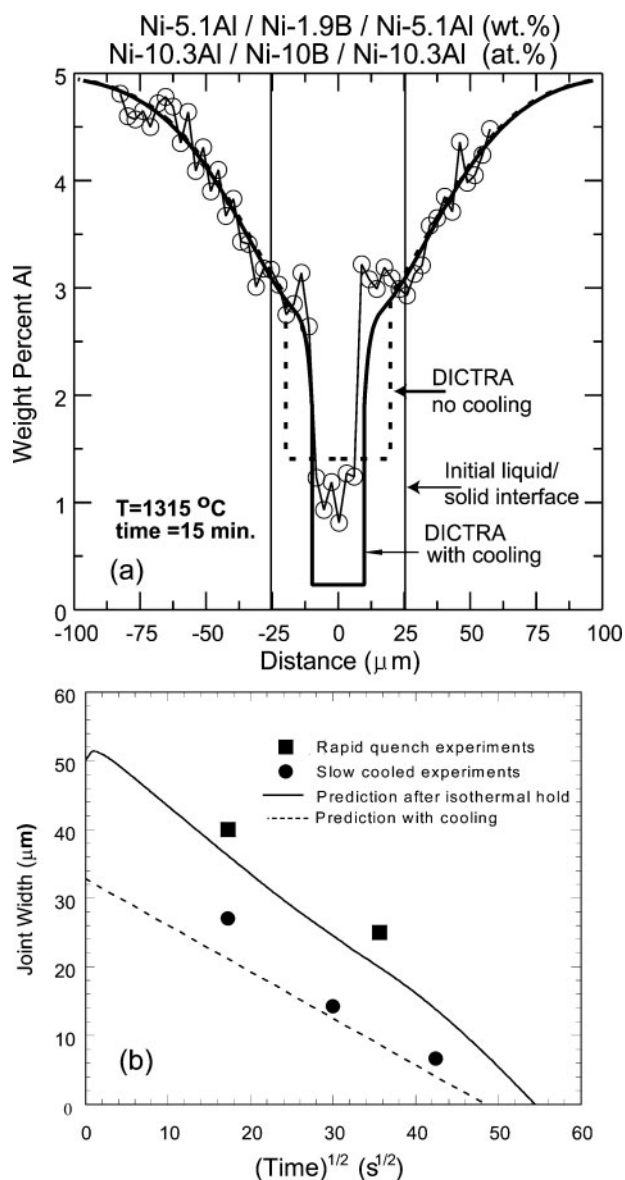
The number of applications where phase equilibria calculations have been directly coupled with other calculations and simulations keeps growing. The diffusion software, described in section on ‘Databases and software tools’, is just one example. Phase equilibria calculations have been incorporated into a finite element package for modelling the solidification of castings¹⁶⁷ and the simulation of freckle formation and macrosegregation in directional solidified Ni base superalloys.¹⁶⁸ The program JMatPro⁷⁶ uses the phase equilibria information to calculate mechanical, thermo-physical and physical properties and phase transformation diagrams.

Diffusion applications

The most common diffusion simulation is the diffusion of one single phase material into another at constant temperature and pressure. The results of these simulations are generally shown as composition profiles as a function of distance at a specified time. The more interesting and industrially relevant diffusion simulations often involve complicated time temperature schedules and the precipitation and dissolution of a variety of different phases. These simulations are characterised by a variety of outputs including the position of a moving phase boundary as a function of time, phase fraction profiles and locations of Kirkendall porosity. These outputs are essential in optimising heat treating cycles and solidification schedules, predicting service lifetimes and determining weldability. (For an updated list of diffusion simulations using DICTRA, please refer to the Thermo-Calc AB website⁸⁵ for references.)



6 *a* a predicted location of maximum pore density for René-N4/René-N5 diffusion couple at 1293°C and *b* backscattered image of René-N4/René-N5 diffusion couple after 100 h at 1293°C: thin white line indicates position of microprobe scan, dashed white line corresponds to Matano interface and other line is location of predicted maximum porosity



7 *a* for TLP bond between Ni-5.1Al and Ni-1.9B, comparison of experimental (symbols) and predicted (solid and dashed lines) Al composition profiles after 15 min at 1315°C (experimental data points are for slow cooled samples and average standard deviation associated with experimental data is 5% of plotted value) and *b* experimental and predicted liquid widths as function of square root of time (standard deviation error associated with each data point is given approximately by symbol size)

The complexity associated with an 11-component Ni base superalloy diffusion couple is demonstrated in Fig. 5 where the interdiffusion between two single phase γ (fcc) Ni base superalloys (René-N4/René-N5) after a 100 h at 1293°C¹⁶⁹ is shown. The predictions were made using the DICTRA software in conjunction with the NIST-NiMob diffusion mobility database¹³² and the ThermoTech Ni Data thermodynamic database.¹⁷⁰ In addition to accurately predicting the composition profiles, the diffusion simulation also predicts the location of the maximum pore formation resulting from Kirkendall porosity. Figure 6*a* shows the predicted location of the maximum pore formation, given by the maximum of the negative derivative of the vacancy flux

with respect to distance,¹⁷¹ and Fig. 6*b* reveals that the predicted location corresponds well to location of Kirkendall porosity observed on the René-N4 side of the diffusion couple.

An example of a moving boundary is shown in Fig. 7. Figure 7*a* shows the calculated and measured composition profiles corresponding to a Ni-Al-B transient liquid phase (TLB) bonding experiment.¹⁷² As isothermal solidification occurs, the transient liquid phase disappears and a bond is formed between the two substrates. Figure 7*b* shows the calculated and measured liquid widths as a function of time. The diffusion simulations are used to predict the correct time temperature profiles to produce TLP bonds which avoid detrimental precipitates.

In an effort to address some of the additional complexities present in multicomponent multiphase 1D diffusion simulations, two additional models have been implemented within the DICTRA code. In applications, such as the processing of cemented carbide tools,¹⁷³ the diffusion path may be blocked by dispersed phase particles. To represent this decreased diffusivity in the matrix, a labyrinth factor, which is a function of volume fraction of the matrix, may be introduced. This model works well for dispersed phases with low volume fractions. As the volume fraction of the dispersed phase increases, validity of the model decreases. A second model implemented by Larsson *et al.*¹⁷⁴⁻¹⁷⁶ treats multiphase diffusion problems when the matrix phase is not continuous. This 1D homogenisation model assumes a system with a constant molar volume and no interstitial components in which the diffusion equations may be solved in the lattice fixed frame of reference. An effective mobility matrix is calculated at each grid point based on the choice of combining rules for determining 'effective' transport properties in multiphase mixtures. The choice of combining rules includes the Wiener¹⁷⁷ and Hashin-Shtrikman¹⁷⁸ bounds. This type of homogenisation model has successfully predicted the diffusion couple profiles for a variety of fcc and bcc multiphase Fe-Cr-Ni diffusion couples¹⁷⁶ and more recently was applied to the interdiffusion occurring between a Ni base superalloy and B2-MCrAlY bond coat.¹⁷⁹

A variety of precipitation programmes, which incorporate matrix diffusion mobilities and thermodynamics using a variety of nucleation, growth and coarsening models, have been^{180,181} or are currently under development.^{182,183} In addition to the thermodynamic and diffusion mobility database inputs, these codes require information on interfacial properties, lattice properties (molar volume) and thermal cycle under which precipitation is occurring. With these inputs, the codes are able to output the time evolution of the precipitation microstructure, including size distributions, number densities and volume fractions and, thus, are able to predict diagrams of time temperature transformation and continuous cooling transformation. Using the CALPHAD method, continued development of composition dependent molar volume¹⁸⁴ and interfacial properties will improve the accuracy of all these precipitation codes.

Materials design

The ultimate integration of multicomponent thermodynamic and diffusion mobility databases is into

materials design tools that enable performance specific materials and processes to be developed. Olson and co-workers have demonstrated how computational thermodynamics and kinetics can be integrated with first principles calculations and experimental results to successfully design a variety of high performance materials, including Nb base superalloys,¹⁸⁵ ultra tough weldable plate steels¹⁸⁶ and stainless steels.¹⁸⁷ These design processes make use of a wide variety of equilibrium and metastable thermodynamic calculations including, but not limited to, calculation of multi-component solid solution temperatures, martensitic start temperatures,¹⁸⁸ paraequilibria¹⁸⁹ and precipitation driving forces.¹⁸⁶ These thermodynamic and kinetic quantities can then be linked with physical and mechanical properties using a variety of software tools.^{186,187,190–193} A more detailed review of computational materials design is given by Kuehmann and Olson¹⁹⁴ in this issue.

Summary

The use of the CALPHAD method in the development of multicomponent thermodynamic and diffusion mobility databases uses a variety of experimental data and first principles calculations as inputs to fit the Gibbs energy and diffusion mobility functions. Using this approach enables efficient storing and accessing of a large amount of experimental data. The ability of the CALPHAD method to extrapolate to higher order systems after accurately defining the needed binary, ternary and when necessary quaternary systems makes it a powerful tool for alloy development and process design. While thermodynamic and diffusion mobility databases have been developed for the major alloy families, work continues to refine these systems, to improve accuracy, and to develop databases for new materials, such as hydrogen storage materials. The currently available thermodynamic and diffusion mobility databases are used in a wide range of applications to predict material properties and microstructure evolution. The development of auxiliary property databases, such as databases for molar volumes of the phases, will enable higher accuracies and an even wider range of applications.

References

1. T. B. Massalski, H. Okamoto, P. R. Subramanian and L. Kacprzak (eds.): 'Binary alloy phase diagrams', 2nd edn, Vols. 1–3; 1990, Materials Park, OH, ASM International.
2. B. Predel: 'Phase equilibria, crystallographic and thermodynamic data of binary alloys', (ed. O. Madelung), Vol. 5; 1991–1998, Landolt-Börnstein, New Series, Berlin, Springer.
3. 'Phase equilibria diagrams', Vols. IX–XIV, compiled in the Ceramics Division of NIST, 1992–2004, Westerville, OH, The American Ceramic Society.
4. 'Phase diagrams for ceramics', Vols. I–VIII, compiled in the Ceramics Division of NIST, 1964–1990, Westerville, OH, The American Ceramic Society.
5. P. Villars, A. Prince and H. Okamoto: 'Handbook of ternary alloy phase diagrams', Vols. 1–10; 1995, Materials Park, OH, ASM International.
6. G. Petzow and G. Effenberg (eds.): 'Ternary alloys: a comprehensive compendium of evaluated constitutional data & phase diagrams', Vols. 1–15; 1988–1995, Weinheim, VCH Verlagsgesellschaft.
7. ASM Alloy Phase Diagram Center: available at: <http://www.as-international.org/asmenterprise/apd/>.
8. Phase Equilibria Diagrams: available at: <http://www.ceramics.org/publications/phase.aspx>.
9. MSIT Workplace/Phase Diagram Center: available at: <http://www.matport.com/workplace/shop/index.shtml>.
10. W. F. Gale and T. C. Totemeier (eds.): 'Smithells metals reference book'; 2004, Amsterdam, Elsevier.
11. H. Bakker, H. P. Bonzel, C. M. Bruff, M. A. Dayananda, W. Gust, J. Horvath, I. Kaur, G. V. Kidson, A. D. LeClaire, H. Mehrer, G. E. Murch, G. Neumann, N. Stolica, and N. A. Stolwijk: in 'Diffusion in solid metals and alloys', (ed. W. Martienssen), Vol. 26, 747; 1990, Berlin, Springer.
12. Diffusion and Defect Forum: available at: <http://www.scientific.net/DDF/>.
13. NIST Diffusion Data Center: available at: <http://patapsco.nist.gov/diffusion/>.
14. J. Hertz: *J. Phase Equilib.*, 1992, **13**, 450–458.
15. L. Kaufman and H. Bernstein: 'Computer calculation of phase diagrams with special reference to refractory metals'; 1970, New York, Academic Press.
16. N. Saunders and A. P. Miodownik: 'CALPHAD: a comprehensive guide'; 1998, Oxford, Pergamon.
17. P. J. Spencer: *CALPHAD*, 2008, **32**, (1), 1–8.
18. J. Ågren: *J. Phys. Chem. Solids*, 1982, **43**, 421–430.
19. J. Ågren: *J. Phys. Chem. Solids*, 1982, **43**, 385–391.
20. J.-O. Andersson and J. Ågren: *J. Appl. Phys.*, 1992, **72**, 1350–1355.
21. B. Jönsson: *ISIJ Int.*, 1995, **35**, 1415–1421.
22. B. Jönsson: *Z. Metallkd.*, 1995, **86**, 686–692.
23. A. Engström and J. Ågren: *Z. Metallkd.*, 1996, **87**, 92–97.
24. M. Hillert: *Physica B*, 1981, **103B**, 31–40.
25. H. L. Lukas, J. Weiss and E.-T. Henig: *CALPHAD*, 1982, **6**, 229–251.
26. A. T. Dinsdale: *CALPHAD*, 1991, **15**, 317–425.
27. J. H. Hildebrand: *J. Am. Chem. Soc.*, 1929, **51**, 66–80.
28. M. Hillert and L.-I. Staffansson: *Acta Chem. Scand.*, 1970, **24**, 3618–3626.
29. M. Hillert and J. Ågren: *Metall. Trans. A*, 1985, **16A**, 261–266.
30. F. Sommer: *Z. Metallkd.*, 1982, **73**, 72–76.
31. M. Blander and A. D. Pelton: *Geochim. Cosmochim. Acta*, 1987, **51**, 85–95.
32. A. D. Pelton and Y.-B. Kang: *Int. J. Mater. Res.*, 2007, **98**, 907–917.
33. C. Wagner and W. Schottky: *Z. phys. Chem. B*, 1930, **11B**, 163–210.
34. W. L. Bragg and E. J. Williams: *Proc. Royal Soc. London A*, 1934, **145A**, 699–730; 1935, **151**, 540–566.
35. O. Redlich and A. T. Kister: *Indust. Eng. Chem.*, 1948, **40**, 345–348.
36. B. Sundman and J. Ågren: *J. Phys. Chem. Solids*, 1981, **42**, 297–301.
37. J.-O. Andersson, A. Fernández Guillermet, M. Hillert, B. Jansson and B. Sundman: *Acta Metall.*, 1986, **34**, 437–445.
38. I. Ansara, T. G. Chart, A. Fernández-Guillermet, F. H. Hayes, U. R. Kattner, D. G. Pettifor, N. Saunders and K. Zeng: *CALPHAD*, 1997, **21**, 171–218.
39. R. Ferro and G. Cacciamani: *CALPHAD*, 2002, **26**, 439–458.
40. I. Ansara, B. Sundman and P. Willemin: *Acta Metall.*, 1988, **36**, 977–982.
41. I. Ansara, N. Dupin, H. L. Lukas and B. Sundman: *J. Alloys Compd.*, 1997, **247**, 20–30.
42. A. Kussolfsky, N. Dupin and B. Sundman: *CALPHAD*, 2001, **25**, 549–565.
43. N. Dupin and I. Ansara: *Z. Metallkd.*, 1999, **90**, 76–85.
44. T. Abe and B. Sundman: *CALPHAD*, 2003, **27**, 403–408.
45. J. M. Sanchez, F. Ducastelle and D. Gratias: *Physica A*, 1984, **128A**, 334–350.
46. A. van de Walle and M. Asta: *Modell. Simul. Mater. Sci. Eng.*, 2002, **10**, 521–538.
47. D. de Fontaine: *Solid State Phys.*, 1994, **47**, 33–176.
48. W. A. Oates and H. Wenzl: *Scr. Mater.*, 1996, **35**, 623–627.
49. G. Inden and W. Pitsch: in 'Materials science and technology', (ed. R. W. Cahn *et al.*) Vol. 5, 497–552; 1991, Weinheim, VCH.
50. A. van de Walle, M. Asta and G. Ceder: *CALPHAD*, 2002, **26**, 519–553.
51. A. van de Walle and G. Ceder: *J. Phase Equilib.*, 2002, **23**, 348–359.
52. W. A. Oates, F. Zhang, S.-L. Chen and Y. A. Chang: *Phys. Rev. B*, 1999, **59B**, 11221–11225.
53. W. Cao, Y. A. Chang, J. Zhu, S. Chen and W. A. Oates: *Intermetallics*, 2007, **15**, 1438–1446.

54. J. Zhu, W. Cao, Y. Yang, F. Zhang, S. Chen, W. A. Oates and Y. A. Chang: *Acta Mater.*, 2007, **55**, 4545–4551.
55. J. Zhang, W. A. Oates, F. Zhang, S.-L. Chen, K.-C. Chou and Y. A. Chang: *Intermetallics*, 2001, **9**, 5–8.
56. F. R. de Boer, R. Boom, W. C. M. Mattens, A. R. Miedema and A. K. Niessen: 'Cohesion in metals'; 1988, Amsterdam, North-Holland.
57. M. S. Daw, S. M. Foiles and M. I. Baskes: *Mater. Sci. Rep.*, 1993, **9**, 251–310.
58. J. Hafner, C. Wolverton and G. Ceder: *MRS Bull.*, 2006, **31**, 659–665.
59. P. E. A. Turchi, I. A. Abrikosov, B. Burton, S. G. Fries, G. Grimvall, L. Kaufman, P. Korzhavyi, V. Rao Manga, M. Ohno, A. Pisch, A. Scott and W. Zhang: *CALPHAD*, 2007, **31**, 4–27.
60. H. L. Lukas, E.-T. Henig and B. Zimmermann: *CALPHAD*, 1977, **1**, 225–236.
61. D. W. Marquardt: *J. Soc. Indust. Appl. Math.*, 1963, **11**, 431–441.
62. E. Königsberger: *CALPHAD*, 1991, **15**, 69–78.
63. H. L. Lukas, S. G. Fries and B. Sundman: 'Computational thermodynamics, the CALPHAD method'; 2007, New York, Cambridge University Press.
64. R. Schmid-Fetzer, D. Andersson, P. Y. Chevalier, L. Eleno, O. Fabrichnaya, U. R. Kattner, B. Sundman, C. Wang, A. Watson, L. Zabdyr and M. Zinkevich: *CALPHAD*, 2007, **31**, 38–52.
65. M. Hillert: *CALPHAD*, 1980, **4**, 1–12.
66. Y.-M. Muggianu, M. Gambino and L. P. Bros: *J. Chim. Phys.*, 1975, **72**, 85–88.
67. M. H. F. Sluiter: *CALPHAD*, 2006, **30**, 357–366.
68. C. W. Bale, P. Chartrand, S. A. Degterov, G. Eriksson, K. Hack, R. B. Mahfoud, J. Melançon, A. D. Pelton and S. Petersen: *CALPHAD*, 2002, **26**, 189–228.
69. R. H. Davies, A. T. Dinsdale, J. A. Gisby, J. A. J. Robinson and S. M. Martin: *CALPHAD*, 2002, **26**, 229–271.
70. S.-L. Chen, S. Daniel, F. Zhang, Y. A. Chang, X. -Y. Yan, F.-Y. Xie, R. Schmid-Fetzer and W. A. Oates: *CALPHAD*, 2002, **26**, 175–188.
71. J.-O. Andersson, T. Helander, L. Höglund, P. Shi and B. Sundman: *CALPHAD*, 2002, **26**, 273–312.
72. H. Yokokawa, S. Yamauchi and T. Matsumoto: *CALPHAD*, 2002, **26**, 155–166.
73. MALT2 (original): available at: <http://www.kagaku.com/malt2/emalt2.html>.
74. B. Cheynet, P.-Y. Chevalier and E. Fischer: *CALPHAD*, 2002, **26**, 167–174.
75. Outotec HSC Chemistry: available at: <http://www.outotec.com>.
76. N. Saunders, Z. Guo, X. Li, A. P. Miodownik and J.-P. Schillé: *JOM*, 2003, **55**, (12), 60–65.
77. U. R. Kattner: *J. Phase Equilib. Diffus.*, 2006, **27**, 126–132.
78. Thermochem Sente Software: available at: <http://www.thermochem.co.uk/>.
79. Scientific Group Thermodata Europe: available at: <http://www.sgte.org>.
80. CompuTherm LLC: available at: <http://www.compuTherm.com>.
81. FactSage: available at: <http://www.factsage.com>.
82. Materials Design Technology: available at: <http://www.materials-design.co.jp/indexE.htm>.
83. MTDATA: available at [http://www.npl.co.uk/\(Home>Science+Technology>Advanced Materials>Materials Areas>Thermodynamics\)](http://www.npl.co.uk/(Home>Science+Technology>Advanced Materials>Materials Areas>Thermodynamics)).
84. NIST Metallurgy Division: available at: <http://www.metallurgy.nist.gov/>.
85. Thermo-Calc Software: available at: <http://www.thermocalc.com/>.
86. I. Ansara, A. T. Dinsdale and M. H. Rand (eds.): 'COST 507 – thermochemical database for light metal alloys', Vol. 2; 1998, Luxembourg, Office for Official Publications of the European Communities.
87. A. Kroupa and J. Vizdal: *Defect Diffus. Forum*, 2007, **263**, 99–104.
88. A. Fick: *Poggendorff's Annalen*, 1855, **94**, 59–86.
89. A. Fick: *Philos. Mag. A*, 1855, **10A**, 30–39.
90. L. Onsager: *Phys. Rev.*, 1931, **37**, 405–426.
91. L. Onsager: *Phys. Rev.*, 1931, **38**, 2265–2279.
92. J. Philibert: *Diffus. Fundam.*, 2006, **4**, 6-1–6-19.
93. M. Koïwa: *Mater. Trans. JIM*, 1998, **39**, 1169–1179.
94. M. Kizilyalli, J. Corish and R. Metselaar: *Pure Appl. Chem.*, 1999, **71**, 1307–1325.
95. J. Philibert: 'Atom movements: diffusion and mass transport in solids', 577; 1991, Les Ulis, Editions de Physique.
96. P. Shewmon: 'Diffusion in Solids', 2nd edn; 1989, Warrendale, PA, TMS.
97. E. O. Kirkendall: *Trans. AIME*, 1942, **147**, 104–110.
98. A. D. Smigelskas and E. O. Kirkendall: *Trans. AIME*, 1947, **171**, 130–142.
99. L. S. Darken: *Trans. AIME*, 1948, **175**, 184–201.
100. L. Boltzmann: *Ann. Phys.*, 1894, **53**, 959–964.
101. C. Matano: *Jpn J. Phys.*, 1933, **8**, 109–113.
102. V. F. Sauer and V. Fries: *Z. Elektrochem.*, 1962, **66**, 353–363.
103. C. Wagner: *Acta Metall.*, 1969, **17**, 99–107.
104. M. A. Dayananda: *Metall. Mater. Trans. A*, 1996, **27A**, 2504–2509.
105. M. A. Dayananda: MultiDiffux Purdue University, 2004, available at: <https://engineering.purdue.edu/MSE/Research/MultiDiFlux/index.htm>.
106. A. Janotti, M. Krcmar, C. L. Fu and R. C. Reed: *Phys. Rev. Lett.*, 2004, **92**, 085901.
107. M. Krcmar, C. L. Fu, A. Janotti and R. C. Reed: *Acta Mater.*, 2005, **53**, 2369–2376.
108. Y. Mishin and D. Farkas: *Philos. Mag. A*, 1997, **75A**, 187–199.
109. Y. Mishin, A. Y. Lozovoi and A. Alavi: *Phys. Rev. B*, 2003, **67B**, 014201.
110. Y. Mishin and C. Herzig: *Acta Mater.*, 2000, **48**, 589–623.
111. Y. Mishin, I. V. Belova and G. E. Murch: *Defect Diffus. Forum*, 2005, **237–240**, 271–276.
112. H. Chamati, N. I. Papanicolaou, Y. Mishin and D. A. Papaconstantopoulos: *Surf. Sci.*, 2006, **600**, 1793–1803.
113. A. van der Ven, G. Ceder, M. Asta and P. D. Tepesch: *Phys. Rev. B*, 2001, **64B**, 184307.
114. H.-C. Yu, D.-H. Yeon, A. van der Ven and K. Thornton: *Acta Mater.*, 2007, **55**, 6690–6704.
115. T. Helander and J. Ågren: *Acta Mater.*, 1999, **47**, 3291–3300.
116. T. Helander and J. Ågren: *Acta Mater.*, 1999, **47**, 1141–1152.
117. J. Kucera and B. Million: *Metall. Trans.*, 1970, **1**, 2603–2606.
118. B. Jönsson: *Z. Metallkd.*, 1994, **85**, 502–509.
119. B. Jönsson: *Z. Metallkd.*, 1992, **83**, 349–355.
120. B. Jönsson: *Z. Metallkd.*, 1994, **85**, 498–501.
121. R. Braun and M. Feller-Kniepmeier: *Scr. Metall.*, 1986, **20**, 7–11.
122. J. Ågren: *Acta Metall.*, 1982, **30**, 841–851.
123. J. Ågren: *ISIJ Int.*, 1992, **32**, 291–296.
124. L. A. Girifalco: *J. Phys. Chem. Solids*, 1964, **24**, 323–333.
125. Z. Tökei, J. Bernardini, P. Gas and D. L. Beke: *Acta Mater.*, 1997, **45**, 541–546.
126. C. E. Campbell: *Acta Mater.*, 2008, **56**, 4277–4290.
127. S. Hallström, L. Höglund and J. Ågren: Presentation at Proc. 6th Euro. Conf. on 'Stainless steel', Helsinki, Finland, June 2008, The Swedish Steel Producers' Association.
128. Thermo-Calc: 'Example i2: Diffusion of carbon in cementite', in 'DICTRA Examples', Version 24 edn; 2006, Stockholm, Sweden, Thermo-Calc AB.
129. M. Hillert, L. Höglund and J. Ågren: *J. Appl. Phys.*, 2005, **98**, 053511.
130. B. Jansson: 'Evaluation of parameters in thermochemical models using different types of experimental data simultaneously', Report TRITA-MAC-0234, Royal Institute of Technology, Stockholm, Sweden, 1984.
131. A. Borgenstam, A. Engström, L. Höglund and J. Ågren: *J. Phase Equilib.*, 2000, **21**, 269–280.
132. C. E. Campbell, W. J. Boettlinger and U. R. Kattner: *Acta Mater.*, 2002, **50**, 775–792.
133. C. E. Campbell: *J. Phase Equilib. Diffus.*, 2005, **26**, 435–440.
134. L. Höglund: unpublished work, DICTRA Toolbox, Thermo-Calc AB, Stockholm, Sweden, 2004.
135. A. M. Brown and M. F. Ashby: *Acta Metall.*, 1980, **28**, 1085–1101.
136. J. R. Manning: *Metall. Trans.*, 1970, **1**, 499–505.
137. C. E. Campbell, J.-C. Zhao and M. F. Henry: *J. Phase Equilib. Diffus.*, 2004, **25**, 6–15.
138. T. Gómez-Acebo, B. Navarcorena and F. Castro: *J. Phase Equilib. Diffus.*, 2004, **25**, 237–251.
139. X. Ma, C. Toffolon-Masclat, T. Guilbert, D. Hamon, J. C. Brachet: *J. Nucl. Mater.*, 2008, **377**, 359–369.
140. Y. L. He, L. Li, S. G. Huang, J. Vleugels and O. van der Bies: *Rare Met.*, 2007, **26**, 492–497.
141. S. Haglund and J. Ågren: *Acta Mater.*, 1998, **46**, 2801–2807.
142. G. Ghosh: *Acta Mater.*, 2001, **49**, 2609–2624.
143. G. Ghosh and Z.-K. Liu: *J. Electron. Mater.*, 1998, **27**, 1362–1366.
144. H. Larsson and J. Ågren: *Comput. Mater. Sci.*, 2005, **34**, 254–263.
145. H. Strandlund and H. Larsson: *Defect Diffus. Forum*, 2004, **233**, 97–133.
146. I. Steinbach, B. Böttger, J. Eiken, N. Warnken and S. G. Fries: *J. Phase Equilib. Diffus.*, 2007, **28**, 101–106.

147. Y. H. Wen, B. Wang, J. P. Simmons and Y. Wang: *Acta Mater.*, 2006, **54**, 2087–2099.
148. K. Wu, Y. A. Chang and Y. Wang: *Scr. Mater.*, 2004, **50**, 1145–1150.
149. J. P. Simmons, Y. Wen, C. Shen and Y. Z. Wang: *Mater. Sci. Eng. A*, 2004, **A365**, 136–143.
150. P.-R. Cha, D.-H. Yeon and J.-K. Yoon: *Acta Mater.*, 2001, **49**, 3295–3307.
151. Q. Chen, N. Ma, K. S. Wu and Y. Z. Wang: *Scr. Mater.*, 2004, **50**, 471–476.
152. K. Asp and J. Ågren: *Acta Mater.*, 2006, **54**, 1241–1248.
153. W. B. Brockman and J. E. Morral: 'Profiler: diffusion couple software to predict concentration profiles'; 1993, Storrs, CT, University of Connecticut.
154. M. S. Thompson and J. E. Morral: *Acta Metall.*, 1986, **34**, 339–346.
155. U. R. Kattner, G. Eriksson, I. Hahn, R. Schmid-Fetzer, B. Sundman, V. Swamy, A. Kussmaul, P. J. Spencer, T. J. Anderson, T. G. Chart, A. Costa e Silva, B. Jansson, B.-J. Lee and M. Schalin: *CALPHAD*, 2000, **24**, 55–94.
156. J. Ågren, F. H. Hayes, L. Höglund, U. R. Kattner, B. Legendre and R. Schmid-Fetzer: *Z. Metallkd.*, 2002, **93**, 128–142.
157. L. Kaufman (ed.): 'User applications of alloy phase diagrams'; 1987, Metals Park, OH, ASM International.
158. F. H. Hayes (ed.): 'User aspects of phase diagrams'; 1991, London, The Institute of Metals.
159. K. Hack (ed.): 'The SGTE casebook, thermodynamics at work'; 1996, London, The Institute of Metals.
160. K.-W. Moon, W. J. Boettinger, U. R. Kattner, C. A. Handwerker and D.-J. Lee: *J. Electron. Mater.*, 2001, **30**, 45–52.
161. S. W. Yoon and H. M. Lee: *CALPHAD*, 1998, **22**, 167–178.
162. W. J. Boettinger and U. R. Kattner: *Metall. Mater. Trans. A*, 2002, **33A**, 1779–1794.
163. H. S. Liu, C. L. Liu, K. Ishida and Z. P. Jin: *J. Electron. Mater.*, 2003, **32**, 1290–1296.
164. W. J. Boettinger, U. R. Kattner, K.-W. Moon and J. H. Perepezko: in 'Methods for phase diagram determination', (ed. J.-C. Zhao), 151–221; 2007, Amsterdam, Elsevier.
165. T. Tanaka, K. Hack and S. Hara: *MRS Bull.*, 1999, **24**, (4), 45–50.
166. R. Pajarre, P. Koukkari, T. Tanaka and J. Lee: *CALPHAD*, 2006, **30**, 196–200.
167. D. K. Banerjee, M. T. Samonds, U. R. Kattner and W. J. Boettinger: in 'Solidification processing 1997', (ed. J. Beech and H. Jones), 354–357; 1997, Sheffield, University of Sheffield.
168. M. C. Schneider, J. P. Gu, C. Beckermann, W. J. Boettinger and U. R. Kattner: *Metall. Mater. Trans. A*, 1997, **28A**, 1517–1531.
169. C. E. Campbell, W. J. Boettinger, T. Hansen, P. Merewether and B. A. Mueller: in 'Complex inorganic solids: structural, stability and magnetic properties of alloys', 241–249; 2005, New York, Springer.
170. N. Saunders: in 'Superalloys 1996', 101–110; 1996, Warrendale, PA, TMS.
171. L. Höglund and J. Ågren: *Acta Mater.*, 2001, **49**, 1311–1317.
172. C. E. Campbell and W. J. Boettinger: *Metall. Mater. Trans. A*, 2000, **31A**, 2835–2847.
173. R. Frykholm, M. Ekroth, B. Jansson, J. Ågren and H.-O. Andren: *Acta Mater.*, 2003, **51**, 1115–1121.
174. H. Larsson, H. Strandlund and M. Hillert: *Acta Mater.*, 2006, **54**, 945–951.
175. H. Strandlund and H. Larsson: *Metall. Mater. Trans. A*, 2006, **37A**, 1785–1789.
176. H. Larsson and A. Engström: *Acta Mater.*, 2006, **54**, 2431–2439.
177. O. Wiener: *Abh. Math. – Phys. Kön. Sächs. Ges. Wis.*, 1912, **32**, 509.
178. Z. Hashin and S. Shtrikman: *J. Appl. Phys.*, 1962, **33**, 3125.
179. K. V. Dahl, J. Hald and A. Horsewell: *Defect Diffus. Forum*, 2006, **258–260**, 73–78.
180. H. J. Jou, P. Voorhees and G. B. Olson: in 'Superalloys 2004', 877–886; 2004, Warrendale, PA, TMS.
181. G. B. Olson, H. J. Jou, J.-W. Jung and J. T. Sebastian: in *Superalloys 2008*, 923–932; 2008, Warrendale, PA, TMS.
182. H. Strandlund, X. Lu, Q. Chen and A. Engström: *Proc. Int. Conf. on 'Materials science and technology'*, 38; 2007, Detroit, MI, American Ceramic Society.
183. K. Wu: *Proc. Int. Conf. on 'Materials science and technology'*, Detroit, MI, 51; 2007, American Ceramic Society.
184. X.-G. Lu, M. Selleby and B. Sundman: *CALPHAD*, 2005, **29**, 68–89.
185. G. Ghosh and G. B. Olson: *Acta Mater.*, 2007, **55**, 3281–3303.
186. A. Saha and G. B. Olson: *J. Comput. Aided Mater. Design*, 2007, **14**, 177–200.
187. C. E. Campbell and G. B. Olson: *J. Comput. Aided Mater. Design*, 2000, **7**, 145–170.
188. G. Ghosh and G. B. Olson: *J. Phase Equilib.*, 2001, **22**, 199–207.
189. G. Ghosh and G. B. Olson: *Acta Mater.*, 2002, **50**, 2099–2119.
190. G. B. Olson: *Science*, 1997, **277**, 1237–1242.
191. Z. K. Liu, L. Q. Chen, P. Raghavan, Q. Du, J. O. Sofo, S. A. Langer and C. Wolverton: *J. Comput. Aided Mater. Design*, 2004, **11**, 183–199.
192. J. Allison, M. Li, C. Wolverton and X. Su: *JOM*, 2006, **48**, (11), 28–35.
193. D. L. McDowell: *JOM*, 2007, **49**, (9), 21–25.
194. C. J. Kuehmann and G. B. Olson: *Mater. Sci. Technol.*, 2009, **25**, 472–478.